Molecular Therapy
Nucleic Acids
Original Article

Adenovirus expressing nc886, an anti-interferon and anti-apoptotic non-coding RNA, is an improved gene delivery vector

Enkhjin Saruuldalai,[1,8] Hwi-Ho Lee,[1,8] Yeon-Su Lee,[2] Eun Kyung Hong,[3] Soyoun Ro,[4] Yeochan Kim,[5] TaeJin Ahn,[5] Jong-Lyul Park,[6,7] Seon-Young Kim,[6,7] Seung-Phil Shin,[4] Wonkyun Ronny Im,[1] Eunjung Cho,[4] Beom K. Choi,[4] Jiyoung Joan Jang,[1] Byung-Han Choi,[1] Yuh-Seog Jung,[4] In-Hoo Kim,[1] Sang-Jin Lee,[4] and Yong Sun Lee[1]

[1]Department of Cancer Biomedical Science, Graduate School of Cancer Science and Policy, National Cancer Center, Goyang 10408, Korea; [2]Division of Rare Cancer, Research Institute, National Cancer Center, Goyang 10408, Korea; [3]Research Institute and Hospital, National Cancer Center, Goyang 10408, Korea; [4]Division of Immuno-Oncology, Research Institute, National Cancer Center, Goyang 10408, Korea; [5]Department of Life Science, Handong Global University, Pohang 37554, Korea; [6]Personalized Genomic Medicine Research Center, KRIBB, Daejeon 34141, Korea; [7]Department of Functional Genomics, University of Science and Technology, Daejeon 34113, Korea

Recombinant adenovirus (rAdV) vector is the most promising vehicle to deliver an exogenous gene into target cells and is preferred for gene therapy. Exogenous gene expression from rAdV is often too inefficient to induce phenotypic changes and the amount of administered rAdV must be very high to achieve a therapeutic dose. However, it is often hampered because a high dose of rAdV is likely to induce cytotoxicity by activating immune responses. nc886, a 102-nucleotide non-coding RNA that is transcribed by RNA polymerase III, acts as an immune suppressor and a facilitator of AdV entry into the nucleus. Therefore, in this study, we have constructed an rAdV expressing nc886 (AdV:nc886) to explore whether AdV:nc886 overcomes the aforementioned drawbacks of conventional rAdV vectors. When infected into mouse cell lines and mice, AdV:nc886 expresses a sufficient amount of nc886, which suppresses the induction of interferon-stimulated genes and apoptotic pathways triggered by AdV infection. As a result, AdV:nc886 is less cytotoxic and produces more rAdV-delivered gene products, compared with the parental rAdV vector lacking nc886. In conclusion, this study demonstrates that the nc886-expressing rAdV could become a superior gene delivery vehicle with greater safety and higher efficiency for *in vivo* gene therapy.

INTRODUCTION

Adenovirus (AdV) is a non-enveloped virus with an icosahedral protein capsid encompassing a linear duplex DNA genome.[1] AdV has long been harnessed as one of the most preferred gene delivery vectors in both basic research and the clinic due to several advantages (reviewed in Lee et al.[2]). AdV is capable of infecting various types of quiescent and proliferating target cells. AdV remains as an episome during transgene expression without integration into the host chromosomal DNA. Thus, unlike other commonly used viral vectors such as retrovirus and lentivirus, AdV is thought to be free of insertional mutations that could lead to cancer. From a safety perspective, there are extensive epidemiological data that AdV infection is not associated with any human disease.[3] Furthermore, the extensive knowledge of AdV biology and genome allows easy manipulation of its genome and massive production of high-titer virions. Because AdV has these advantages over other viral vectors such as adeno-associated virus (AAV), retrovirus, and lentivirus, a large number of recombinant AdVs (rAdVs) have been introduced to carry transgenes and have been translated into clinical trials, mainly in gene therapy for monogenic diseases.[4]

Gene expression and replication of wild-type AdV occur within the host cell nucleus, where they produces millions of viral progenies by hijacking the host gene expression machinery, resulting in host cell lysis and release of progeny virions. When used for gene therapy, these events are certainly undesirable and are avoided by deleting E1 genes essential for AdV replication.[2] Nevertheless, such replication-defective rAdVs are still cytotoxic, mainly due to immune responses elicited by infected cells and immune cells around them. The innate immune system in host cells senses incoming AdVs and secretes cytokines and chemokines.[5,6] An important class of these are type I interferons (IFNs), which initiate a signaling cascade for the transcriptional activation of hundreds of IFN-stimulated genes (ISGs).[7,8] These ISGs play important roles in mounting anti-viral defenses, stimulating adaptive immunity, and inducing apoptosis.[6,7,9] These

Received 4 April 2024; accepted 12 July 2024;
https://doi.org/10.1016/j.omtn.2024.102270.

[8]These authors contributed equally

Correspondence: Sang-Jin Lee, Division of Immuno-Oncology, Research Institute, National Cancer Center, Goyang 10408, Korea.
E-mail: leesj@ncc.re.kr
Correspondence: Yong Sun Lee, Department of Cancer Biomedical Science, Graduate School of Cancer Science and Policy, National Cancer Center, Goyang 10408, Korea.
E-mail: yslee@ncc.re.kr

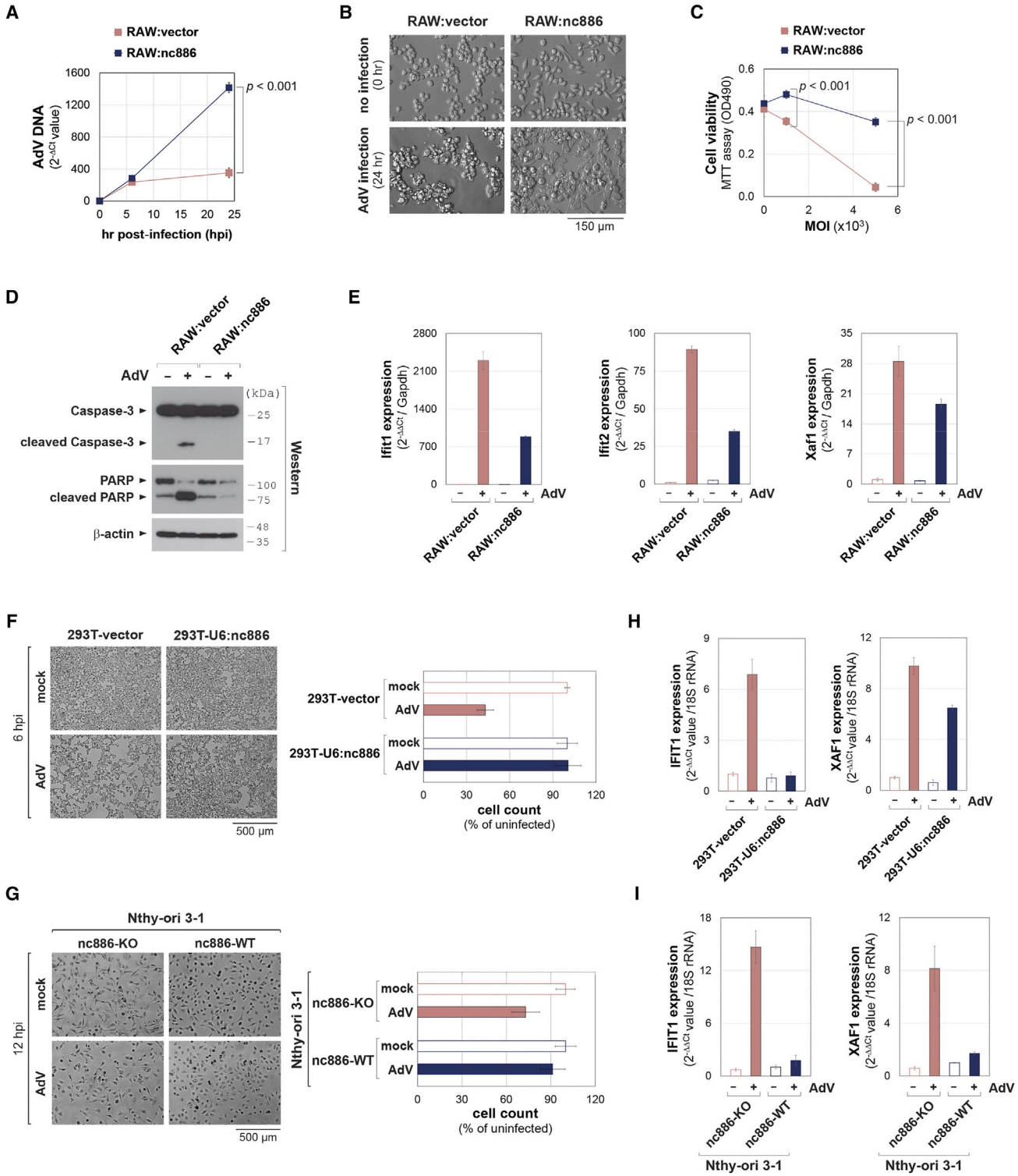

Figure 1. Mitigation of AdV-mediated cytotoxicity by nc886

(A) qPCR of AdV DNA from AdV5-infected samples at 1,000 MOI. Expression values (as indicated on the y axis) are plotted, with the value of uninfected RAW:vector being set to 1. This experiment was repeated twice with three technical replicates in each experiment. A representative biological replicate is shown. Error bars represent the mean ± SD of technical replicates. (B) Representative images of cells before and at 24 hpi of AdV5 at 1,000 MOI. (C) Measurement of cell viability by MTT assays at 24 hpi of AdV5 at

(legend continued on next page)

responses are originally beneficial to the host but turn into a serious threat to the host when they become uncontrollable, resulting in massive release of cytokines (termed "cytokine storm"). Most people have pre-existing immunity to AdV, which limits incoming rAdV and consequently lowers the expression of a transgene from rAdVs.[10] As a result, in gene therapy, rAdV is administered at high doses to achieve sufficient expression of a therapeutic gene. However, such a high dose of rAdV may inadvertently induce too much IFN. There was a case where rAdV caused a cytokine storm and the death of a patient during a gene therapy clinical trial.[11] Therefore, it is imperative to control immunity during AdV-mediated gene therapy.

nc886 is a 102 nucleotide (nt) long human non-coding RNA (ncRNA) that is transcribed by RNA polymerase III (Pol III).[12] Several roles of nc886 have been reported, and the best studied being the suppression of an antiviral and pro-apoptotic protein called protein kinase R (PKR).[13] By inhibiting the activity of PKR and other innate immune pathways, nc886 suppresses the production of cytokines such as IFN-β, IFN-γ, and interleukin-2 (IL-2).[14,15] Recently, we have shown that nc886 is required for AdV replication. Although we initially thought that this requirement is due to the immunosuppressive function of nc886, our detailed investigation revealed that nc886 facilitates AdV replication not by controlling immunity but by promoting AdV nuclear trafficking, an initial step in the AdV life cycle.[16] This finding explains why human AdV (hAdV) replicates poorly in mouse cells lacking an nc886 ortholog. nc886's role as an IFN suppressor and pro-AdV factor motivated our study here to use nc886 in AdV-mediated gene delivery and ultimately for future gene therapy.

RESULTS

nc886 mitigates a cytotoxic effect of AdV on target cells

As mentioned in the introduction, the propagation of hAdV is very inefficient in mouse cells lacking nc886.[17–20] In our previous study,[16] we generated a derivative cell line expressing nc886 (hereafter designated "RAW:nc886") and a control cell line ("RAW:vector") from RAW 264.7 mouse macrophage cells. Upon infection with hAdV, more AdV DNA was detected in RAW:nc886 cells than in RAW:vector cells (Figure 1A), consistent with our previous finding that nc886 promotes AdV nuclear trafficking.[16] During infection of these cells, we also observed a cytotoxic effect of AdV (Figures 1B and 1C). This cytotoxicity was accompanied by apoptosis, as demonstrated by cleavage of caspase-3 and PARP (Figure 1D), consistent with a previous paper that observed apoptosis upon AdV infection.[21] Notably, RAW:nc886 cells exhibited better cell survival and less apoptosis than RAW:vector cells, despite more AdV entry (Figures 1B–1D).

Since hAdV replication is defective in mouse cells, the infected AdV (Figures 1A–1D) could not have completed its life cycle and were unable to release progeny virions through lysis of infected cells. Therefore, the cytotoxicity seen in Figures 1B–1D was most likely to result from the input AdV, not from progeny virions. In support of this idea, AdV-mediated cytotoxicity, as indicated by the difference in cell density, was evident before ∼24 h post-infection (hpi) and this time point is much earlier than the production of progeny virions.[23] Because of the replication defect, we had to administer hAdV at a high multiplicity of infection (MOI) in this experiment to measure post-infection outcomes such as AdV gene expression. Taken together, we hypothesized that the cytotoxicity was caused by immune responses and that the higher number of surviving RAW:nc886 cells was due to nc886's immunosuppressive function. Indeed, ISGs such as Ifit1, Ifit2, and Xaf1 were dramatically induced in RAW:vector cells upon AdV infection and this induction was lower in RAW:nc886 cells (Figure 1E).

We interrogated whether nc886 mitigated the cytotoxicity upon AdV infection also in human cells. HEK293T (shortly "293T") is an nc886-silenced cell line, from which we had constructed an nc886-expressing derivative cell line (designated "293T-U6:nc886") and a control cell line ("293T-vector").[24] An nc886 knockout (KO) cell line was generated from a thyroid cell line, Nthy-ori 3-1, which naturally expresses nc886 (hereafter referred to as nc886-KO and nc886-WT, respectively).[22] In these two pairs of cell lines, AdV was infected at high MOIs and cells were observed before AdV replication, similarly to the experimental condition for mouse cells in Figures 1A–1E. Input AdV resulted in fewer viable cells when infected to 293T-vector and Nthy-ori 3-1 nc886-KO cell lines (Figures 1F and 1G). Importantly, this cytotoxicity was attenuated when nc886 was expressed, as indicated by increased cell numbers in 293T-U6:nc886 and Nthy-ori 3-1 (nc886-WT) cell lines (Figures 1F and 1G). The expression of two ISGs, IFIT1 and XAF1, was induced upon AdV infection and this induction was less in the nc886-expressing cell lines than in nc886-silenced or -null counterparts (Figures 1H and 1I). Taken together, these data suggest that AdV and nc886 affect immune responses and cytotoxicity in a similar manner in mouse and human cells.

An rAdV-expressing nc886 is less cytotoxic than its parental AdV

The experimental condition in Figure 1 was high-dose AdV infection and, as a result, induction of cytotoxicity by non-replicated input AdV via excessive induction of ISGs. Notably, this experimental condition mimics a situation that occurs during the infusion of AdV into humans for gene therapy. The results in Figure 1 inspired us with the

indicated MOIs. This experiment was repeated twice with three technical replicates in each experiment. A representative biological replicate is shown. Error bars represent the mean ± SD of technical replicates. (D) Western blot of apoptotic markers at 24 hpi of AdV5 at 1,000 MOI. (E) qRT-PCR of the indicated ISGs. Expression values normalized to Gapdh are plotted, with the value of uninfected RAW:vector being set to 1. Data are presented as the average of three technical replicates. Error bars represent the mean ± SD. (F and G) Representative images of cells at 10× magnification. Indicated cell lines were either mock infected (with vehicle) or infected with AdV5 at 200 MOI for 6 h (F) and 500 MOI for 12 h (G). In the Nthy-ori 3-1 pair, "nc886-KO" indicates cells with double KO of nc886 and PKR (see Lee et al.[22] for details). Cells were counted from randomly selected quintuplicate fields at 40× magnification (F) and at 20× magnification (G). Average values are plotted on the right, with values of uninfected cells being set to 100%. Error bars represent the mean ± SD. (H and I) qRT-PCR of the indicated ISGs. Expression values normalized to 18S rRNA are plotted, with the value of uninfected 293T-vector or Nthy-ori 3-1 nc886-KO cells being set to 1. Data are presented as the average of three technical replicates. Error bars represent the mean ± SD.

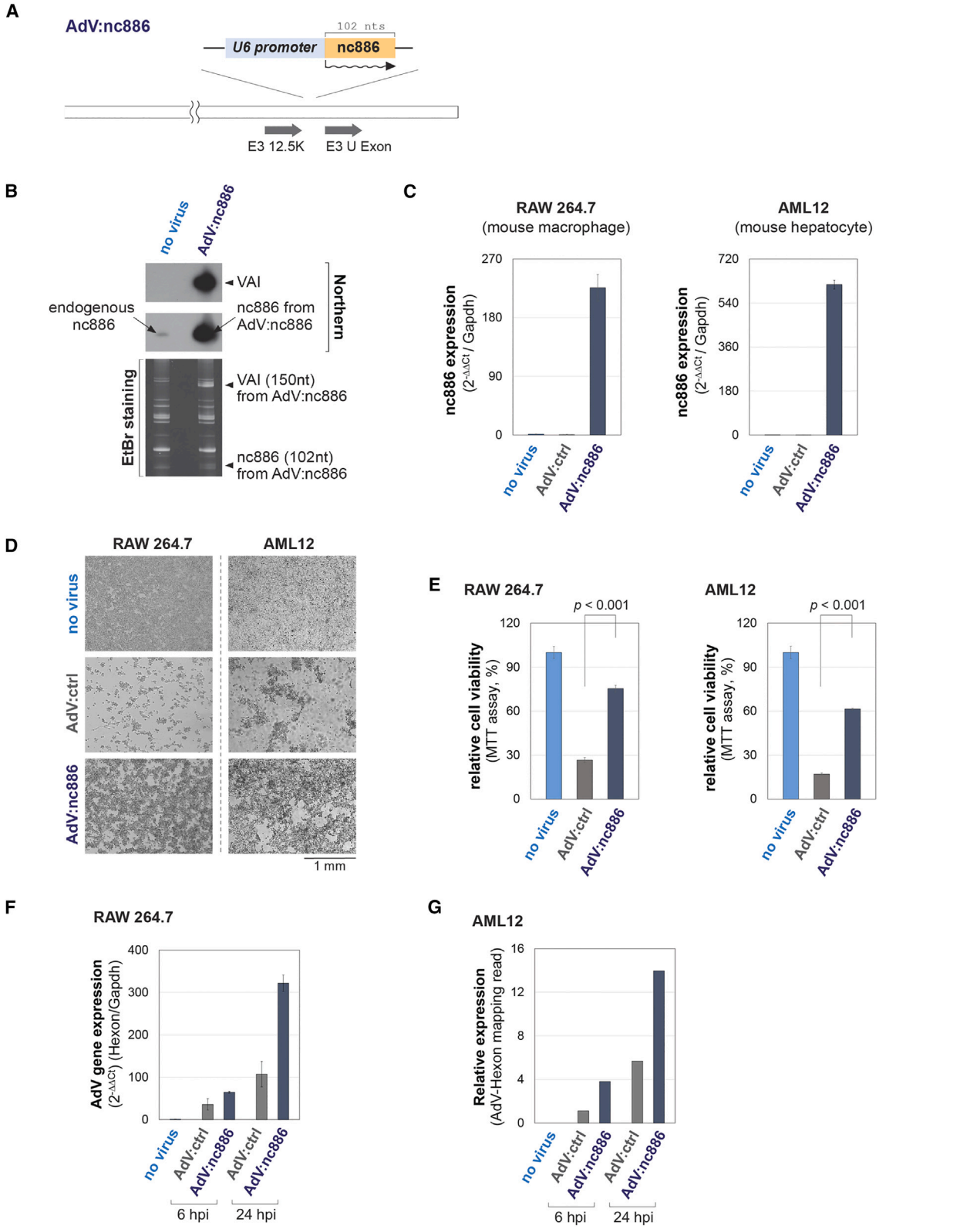

(legend on next page)

idea to express nc886 from infected AdV. Such an nc886-expressing rAdV might be useful in AdV-mediated gene therapy by alleviating the damage to target cells. To realize this idea, we inserted the nc886 gene into the AdV genome to construct an rAdV to express nc886 (hereafter referred to as "AdV:nc886").

To achieve the abundant and constitutive expression of nc886 from AdV:nc886, we considered which Pol III promoter to use. As a Pol III-transcribed ncRNA, nc886 is abundantly expressed from its natural promoter.[12] Although such abundant expression is desirable, the activity of the nc886 promoter is highly variable due to extensive regulation by epigenetic mechanisms and transcription factors.[25] To achieve constitutive expression, we chose an external promoter for small nuclear RNA U6 ("U6 promoter"), which is an invariably expressed Pol III-transcribed ncRNA. nc886 was cloned under the U6 promoter and then the U6:nc886 cassette was inserted into the E3 region of the parental AdV (an AdV strain AdV5/35; designated "AdV:ctrl" hereafter) as illustrated in Figures 2A and S1.[26]

First, we validated the efficient expression of nc886 from AdV:nc886 by infecting a human cell line. Our northern blot showed abundant expression of nc886 from AdV:nc886-infected samples (right lane in Figure 2B). The intensity of this signal was much stronger than that of the endogenous nc886 expressed by the human host cells (uninfected sample, left lane in Figure 2B). This discrepancy could be explained by the difference in DNA copy number. Since this experiment was performed in a replication-competent condition, AdV:nc886 was likely to have replicated in the human host cells post viral entry and thus multiplied copies of AdV:nc886 DNA in the nucleus served as a transcriptional template. In comparison, the endogenous nc886 was transcribed from only two copies of human genomic DNA. Therefore, it would be fair to compare the expression of nc886 with other AdV-encoded genes such as a Pol III-transcribed ncRNA called virus-associated I (VAI).[27] In the ethidium bromide staining shown in Figure 2B, both nc886 and VAI bands of comparable intensity were visible only in the "AdV:nc886"-infected sample and not in "no-virus" sample.

Next, we tested whether nc886 expressed from AdV:nc886 is effective in mitigating cytotoxicity in the *in vitro* experimental condition similar to AdV-mediated gene therapy. For this, RAW 264.7 and a mouse hepatocyte cell line (AML12) were infected with a high dose of AdV. In both of these cell lines, AdV:nc886 expressed nc886 (Figure 2C) and, importantly, induced less cytotoxicity than AdV:ctrl (Figures 2D and 2E). To exclude a possibility that AdV:nc886 might have poorly infected these cells and therefore was less cytotoxic, the expression of an AdV gene Hexon was measured by qRT-PCR for RAW 264.7 and was estimated by high-throughput sequencing of total RNA (RNA-seq) for AML12. The Hexon mRNA level was higher in AdV:nc886 than in AdV:ctrl (Figures 2F and 2G), clearly demonstrating that AdV:nc886-infected cells were less toxic despite more AdV gene expression.

AdV:nc886 elicits less tissue damage and higher AdV gene expression in mice

The *in vitro* experimental data shown in Figure 2 were encouraging, and we proceeded to investigate equity in mice. C57BL/6 mice were intravenously infected with AdV via tail-vein, according to the experimental design and schedule shown in Figure 3A. After sacrifice, the viral toxicity was assessed in blood and in liver tissue, in which AdV is known to be mainly detected after systemic administration.[28] nc886 expression was detected only in the group of mice injected with AdV:nc886 (Figure 3B).

Systemic administration of AdV is known to cause acute inflammation and liver injury, which hamper AdV-mediated gene therapy from a safety perspective.[29,30] We examined potential liver tissue damage by histopathological analysis of liver paraffin sections stained with hematoxylin and eosin (H&E). Numerous scans of spotty necrosis clusters (indicated by black arrows in the left panel of Figure 3C), an indicator of hepatocyte damage, were observed in the AdV:ctrl-injected group. This tissue damage was undoubtedly caused by AdV infection, as it was not seen in the no-virus control group. Importantly, these spotty necrosis clusters were significantly decreased in the mice group injected with AdV:nc886 (Figure 3C). We also measured serum levels of glutamic pyruvic transaminase (GPT) and glutamic oxaloacetic transaminase (GOT), which are indicators of liver damage.[31] Consistent with the H&E staining of liver tissue, GPT and GOT enzymatic activities were elevated in the AdV:ctrl-injected group compared with the no-virus control group and these GPT and GOT elevations were attenuated in the mice group injected with AdV:nc886 (Figure 3D).

To evaluate the efficiency of gene expression delivered by AdV, total RNA was isolated from liver tissue and the amount of an AdV mRNA was measured. The expression level was significantly higher

Figure 2. Construction and validation of nc886-expressing AdV and its efficacy in mitigating cytotoxicity and expressing an AdV gene

(A) A simplified cartoon depicting the insertion of the U6:nc886 cassette into the parental AdV (which is "AdV:ctrl"). See Figure S1 for a full map. (B) Northern hybridization of nc886 and AdV VAI RNA after infection of AdV:nc886 (at 10 MOI for 24 h) into a human cell line (293T cells made to express nc886). Ethidium bromide (EtBr) staining is to ensure equal loading and to show EtBr-stainable nc886 and VAI bands. (C) qRT-PCR of nc886. Cells were infected with the indicated AdVs at 100 MOI for 6 h. Normalized values (to the mouse Gapdh gene) are plotted with uninfected ("no virus") samples being set to 1. Error bars represent the mean ± SD. (D) Representative images of cells infected with AdVs as indicated. Infections into RAW 264.7 and AML12 were at 100 MOI for 72 h and at 50 MOI for 148 h, respectively. (E) Quantitation of cells in (D) by MTT assays. MTT values are plotted with uninfected ("no virus") samples being set to 100%. This experiment was repeated twice with three technical replicates in each experiment. A representative biological replicate is shown. Error bars represent the mean ± SD of technical replicates. (F) qRT-PCR of AdV Hexon mRNA from RAW 264.7 cells infected with the indicated AdVs at 100 MOI. Data normalization and plotting are as described in (C). Data are presented as the average of three technical replicates. Error bars represent the mean ± SD. (G) Relative RNA-seq reads mapped to AdV Hexon mRNA from AML12 cells infected with indicated AdVs at 100 MOI. Raw read values were normalized to the total reads, multiplied by an arbitrary value (10^6), log2 transformed, and plotted.

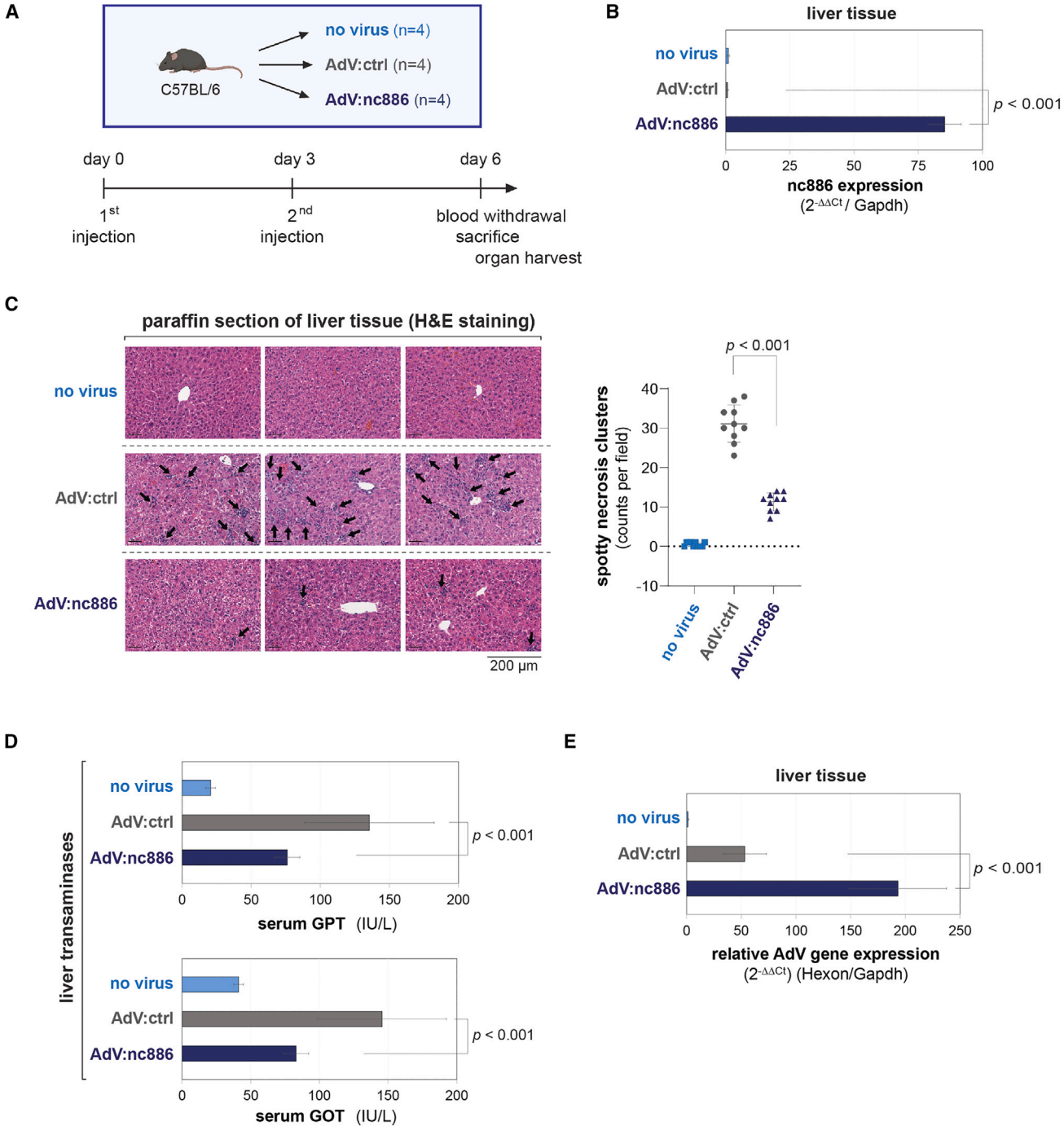

Figure 3. Reduced tissue damage and increased AdV gene expression in mice injected with AdV:nc886

(A) A cartoon (created with BioRender.com) for the systemic administration of AdV to mice, showing the experimental design such as experimental sets, the number of mice, and a timeline. (B) Measurement of nc886 in liver tissue by qRT-PCR. Each bar represents an average of 12 values (triplicate samples from each of four mice). Data normalization and plotting are as described in Figure 2C. (C) Representative images of H&E-stained mouse liver paraffin sections at 10× magnification, with black arrows pointing spotty necrosis clusters indicative of damaged/apoptotic hepatocytes. The number of these clusters per field of view was counted at 4× magnification. Counts from ten fields per a group are plotted on the right. (D) The level of transaminases (GPT and GOT) in serum. Each bar represents an average of 12 values (triplicate samples from each of four mice). IU/L, international units per liter. Error bars represent the mean ± SD of 12 values. (E) qRT-PCR of AdV Hexon mRNA in liver tissue. All descriptions are the same as (B).

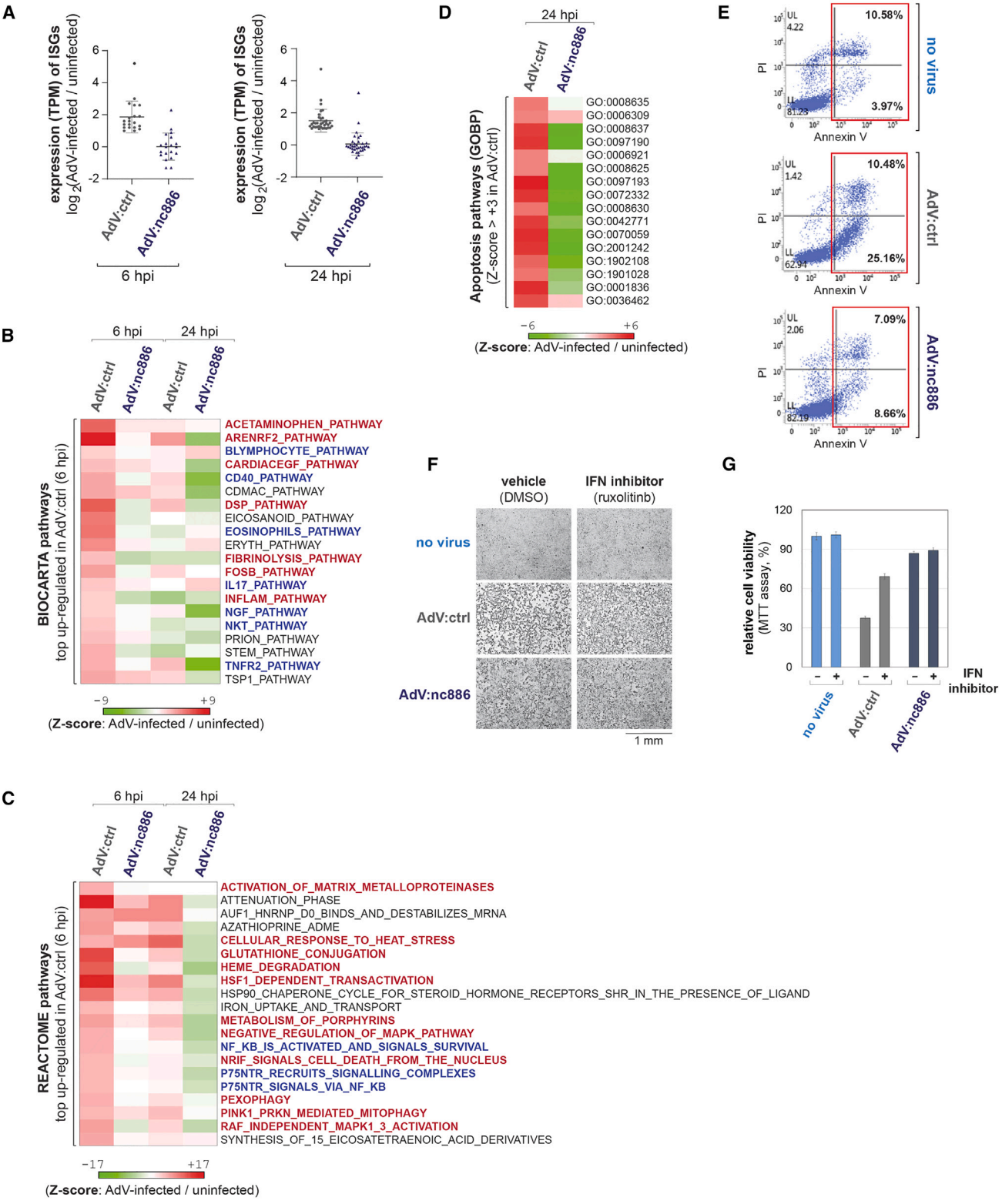

(legend on next page)

in the mice group injected with AdV:nc886 than in the group with AdV:ctrl (Figure 3E). This result is not only important in itself but also provides evidence that the reduced tissue damage in the AdV:nc886-treated mice (Figures 3C and 3D) was not due to inefficient delivery to the liver or poor infection of hepatocytes. In conclusion, our mouse experiments with AdV:nc886 demonstrated the beneficial properties of nc886 expression in AdV-mediated gene delivery *in vivo*.

The lower cytotoxicity of AdV:nc886 is attributed to nc886's immunosuppressive function

AdV infection triggers innate immune cascades to induce the expression of ISGs.[32,33] nc886 is capable of controlling gene expression[12–15,34] and is hypothesized to modulate immune responses via its gene-regulatory function. We investigated the AdV-mediated change in gene expression and the role of nc886 in this process, with the aim of finding the underlying reasons for the superiority of AdV:nc886, which would be important information from a safety viewpoint. Our tissue analyses from mouse experiments (in Figure 3) was focused on the liver, which is the major target organ by intravenous injection of AdV *in vivo*.[35] Therefore, AML2 mouse hepatocyte cells were selected for gene expression analysis. After infection with AdV:nc886 or AdV:ctrl, we performed RNA-seq to obtain global gene expression profiles.

Our initial analysis focused on ISGs. We retrieved a list of 376 ISGs[8] and examined them in our RNA-seq data (Tables S1 and S2). First, we eliminated negligibly expressed ISGs whose transcripts per million (TPM) values were less than 1. Then, we selected ISGs whose TPM value was >2-fold induced by AdV:ctrl compared with the uninfected sample. This yielded 20 and 35 ISGs in the 6 and 24 hpi samples, respectively. For each of these ISGs, hereafter referred to as "AdV-induced ISGs," fold-change values (AdV-infected/uninfected) were calculated and displayed on a dot plot (Figure 4A). The expression levels of these AdV-induced ISGs were significantly lower in AdV:nc886-infected samples than in AdV:ctrl-infected samples. These data indicate that nc886 suppresses the AdV-induced IFN response in addition to that induced by RNA viruses or synthetic RNA as previously shown in human cells.[14,15] These results (Figure 4A), together with our earlier results in Figures 1E, 1H, and 1I, indicate that the suppression of IFN by nc886 is effective not only in human cells but also in mouse cells despite the absence of a mouse nc886 ortholog.

Next, we sought to identify which biological processes and pathways were altered by AdV and controlled by nc886. To this end, we analyzed the RNA-seq data in the Molecular Signature Database (Database: https://www.gsea-msigdb.org/gsea/msigdb), which contains several pathway sets such as Biocarta (consisting of 252 pathways, see Table S3) and Reactome (consisting of 1,261 pathways, Table S4). By comparing gene expression data of AdV-infected samples to the uninfected sample, we calculated a *Z* score of each pathway, a value indicating activation or suppression upon AdV infection. We obtained *Z* scores for 252 Biocarta pathways and 1,261 Reactome pathways, sorted them in descending order, and selected the top 20 pathways. By analyzing the AdV:ctrl-infected sample at 6 hpi, we collected the most activated pathways by AdV at a relatively early time point before cytotoxicity was manifested.

Looking at each of these 20 pathways (Figures 4B and 4C; Tables S3 and S4), a majority of them were involved in immunity in a broad sense (highlighted with bold blue letters), as expected. There were also pathways related to liver inflammation and damage (bold red letters), which was the phenomenon consistent with what we observed in liver tissue after AdV infusion into mice. Most importantly, the comparison between AdV:nc886 and AdV:ctrl on the heatmap (Figures 4B and 4C) clearly showed that most of these pathways were suppressed by nc886.

The key advantage we expected from adding nc886 to an AdV vector was a reduced toxicity to infected cells. Our experiments (Figures 2 and 3) clearly showed reduced cytotoxicity, such as less necrosis of liver tissue in mice and more surviving cells *in vitro* when treated with AdV:nc886. We sought to provide a basis for these phenotypes by analyzing gene expression data. Our data showed that nc886 suppressed the expression of AdV-induced ISGs (Figure 4A). According to previous studies, IFN has an apoptotic activity via the induction of ISGs,[9,36] and apoptotic gene signatures are predictable markers of liver necrosis.[37] Taken all these together, further analysis was performed focusing on apoptosis by examining apoptosis-related pathways from the mouse Gene Ontology Biological Process (GOBP) set, which contains 10,662 biological processes (Table S5). We calculated *Z* scores for each of them, made a shortlist of biological processes that were activated (*Z* score > +3) by AdV-ctrl (relative to uninfected) at 24 hpi, and manually selected 16 apoptosis-related pathways. Most of them had lower *Z* scores in AdV:nc886 than in AdV:ctrl, as clearly shown in the heatmap (Figure 4D). The effect

Figure 4. Weaker induction of IFN responses and the resultantly lower apoptosis in AdV:nc886-infected cells

(A) Dot plots displaying the fold induction of expression of AdV-induced ISGs in AML12 cells (see the main text for details), which was calculated from TPM values in RNA-seq data. (B and C) Heatmaps showing *Z* scores of the top 20 upregulated pathways in AdV-infected samples at 6 hpi (relative to the "uninfected" sample) in the BIOCARTA (B) and the REACTOME (C) sets, across the four samples indicated at the top. A color scale bar is shown at the bottom. (D) A heatmap showing *Z* scores of apoptosis-related GOBPs that were significantly induced by the infection of AdV:ctrl (see the main text for details). For each of GOBPs, its GO identifier number is indicated on the right and its GO name is in Table S5. (E) Annexin V and propidium iodide (PI) staining of AdV-infected AML12 cells at 70 hpi of AdV5 at 500 MOI. Annexin V-positive apoptotic cells are shown in red boxes, with the corresponding percentage. (F and G) Representative images (F) and MTT assays (G) of cells treated with 4 μM ruxolitinib (or DMSO as a vehicle control) in combination with infection of indicated AdVs at 100 MOI. Drug treatment at 0 h and then AdV infection at 2 h were followed by cell photos taken and MTT assays at 50 h. MTT values are plotted, with the uninfected and vehicle-treated sample being set to 100%. n.s., not significant. Data are presented as the average of three technical replicates. Error bars represent the mean ± SD.

of AdV and nc886 on apoptosis was experimentally validated by annexin V/propidium iodide staining after infection to AML12 cells. Compared with no-virus control, a significant proportion of AdV:ctrl-infected cells underwent apoptosis and this apoptotic population was clearly lower in the AdV:nc886-infected sample (Figure 4E).

Our pathway analysis suggested that nc886 expressed from AdV:nc886 attenuated AdV-mediated cytotoxicity by suppressing IFN responses. To further prove this, AML12 cells were treated with ruxolitinib followed by AdV infection. Ruxolitinib, an IFN inhibitor, is known to suppress ISG expression by targeting the Janus kinase-signal transducers and activators of the transcription signaling pathway.[38] Ruxolitinib-treated cells survived better than control cells after infection with AdV:ctrl (Figures 4F and 4G), demonstrating that AdV-mediated cytotoxicity was, at least partly, due to IFN responses. In contrast, ruxolitinib had almost no effect on AdV:nc886-infected cells (Figures 4F and 4G), presumably because IFN responses were already suppressed by nc886 and thus there was no need for an IFN inhibitor. These data demonstrate that the low cytotoxicity of AdV:nc886 is due to the suppressive effect of nc886 on IFN.

DISCUSSION

In this study, we construct AdV:nc886 and demonstrate its advantages as a gene delivery vector. Our data show that AdV:nc886 efficiently expressed nc886, which suppressed AdV-induced IFN responses, thereby alleviating the cytotoxicity caused by AdV infection. In addition, the gene expression delivered by AdV:nc886 was higher than that of AdV:ctrl, as consistently shown in our experiments with a magnitude ranging from 2- to 4-fold. It should be noted that this magnitude was obtained by measuring AdV transcripts from the same amount of total RNA. Given that more cells survived after AdV:nc886 infection, the magnitude of the difference will be much higher if calculated from the initial amount of tissue or cells subjected to AdV infection. In conclusion, AdV gene expression data strongly suggest that AdV:nc886 could be a superior vector that more efficiently expresses a therapeutic gene when used in AdV-mediated gene therapy.

There are several possible reasons for the better gene expression from AdV:nc886 than from AdV:ctrl. One simple possibility is that AdV:nc886-infected cells are healthier and therefore more transcriptionally active. Another possibility is the role of nc886 in facilitating AdV import into the nucleus, as reported in our previous study.[16] This mechanism is not operative during initial infection because trafficking precedes the transcription of nc886 from AdV:nc886. At later time points, nc886-expressing cells will accumulate after AdV:nc886 infection. When these cells are re-infected, they may be better able to import AdV into the nucleus and consequently express more AdV genes.

Although we have performed most of the *in vitro* cell and *in vivo* animal experiments in mice, we expect that the benefits of AdV:nc886 will also be extrapolated to humans. Our animal experiments focused on the liver (Figure 3), which would also be the primary target organ for AdV when systemically injected in humans, where approximately 1.5 L of blood per minute is delivered from the portal vein and hepatic artery into the liver sinusoids for filtration. Therefore, liver-directed gene therapy would be the first choice if AdV:nc886 is used in human clinical trials. For broad application, future studies should evaluate the benefit of AdV:nc886 in other organs. Regarding nc886 and IFN, our previous study showed that nc886 suppresses IFN responses in human cells when induced by RNA viruses or synthetic pathogenic RNA. Although the triggers are different, it is highly likely that nc886 also suppresses AdV-induced IFN responses in human cells similarly to mouse cells. Studies in human cells have shown that IFN responses are activated by AdV through the retinoic acid-inducible gene I pathway,[33] which is also critical when nc886 inhibits IFN in human cells.[14] Indeed, our experiment showed that at least two ISGs were induced by AdV and that this induction was suppressed by nc886 (Figures 1H and 1I). To apply AdV:nc886 in clinical use in humans, it is necessary to know how similar AdV-mediated IFN responses are between human and mouse cells. To this end, our future study will comprehensively measure human ISGs by RNA-seq and compare with mouse data.

AdV is still the most commonly used delivery vehicle for gene therapy, currently accounting for 50% of all viral-based clinical trials worldwide.[39] However, AdV induces a strong immune response and cytotoxicity in target cells (see introduction and Figures 1, 2, 3, and 4), and therefore AAV vectors have recently been considered as an alternative. Although the cellular immune response upon AAV infection is weak compared with AdV,[40] the packaging capacity of AAV is approximately 7–8 times smaller than that of AdV. In addition, recent reports on AAV clinical trials warn that AAV may be oncogenic.[41,42] To the best of our knowledge, there are no epidemiologic data that AdV infection is associated with any human disease. Therefore, the improvement of AdV, which should be directed toward clinical implementation for favorable patient outcomes, deserves more attention. There have been several reports about strategies to insert immune-suppressing genes, such as suppressor of cytokine signaling-1 (SOCS1)[43] and IL-10,[44] into the AdV genome with promising results. These are protein-coding genes that are transcribed by RNA polymerase II (Pol II) and we want to highlight the unique advantages of nc886 over these. The U6:nc886 cassette is short (417 nt) and thus its insertion hardly occupies the coding capacity of the AdV genome, which is ~35 kilobase long. The U6:nc886 cassette is an independent transcription unit and can therefore be inserted almost anywhere in the AdV genome. Transcription by Pol III makes this cassette truly independent, with minimal interference with neighboring AdV genes or a therapeutic transgene, which are mostly transcribed by Pol II. When a Pol II-transcribed gene such as SOCS1 or IL-10 is inserted, it can affect or be affected by nearby genes; for example, by generating read-through transcripts or by competing with Pol II enzymes. As a Pol III gene, nc886 is free from this potential problem. In addition, the constitutive U6 promoter will drive nc886 transcription in most infected cells.

In addition to its potential in gene therapy, AdV:nc886 could also be used in vaccine development and oncolytic therapy. For vaccine applications, we expect AdV:nc886 to be a safer vector that delivers an antigen efficiently for a longer period of time due to the advantages demonstrated in this study, including attenuated IFN responses, reduced cytotoxicity, and enhanced gene expression. While AdV-mediated delivery of therapeutic genes or antigens occurs in a non-replicating state, oncolytic therapy is based on the lysis of infected cells at the end of the AdV life cycle.[45] Also in this case, AdV:nc886 will be superior because nc886 is a positive factor in the AdV life cycle by facilitating the nuclear trafficking of AdV.[16] Although AdV:nc886 will not be advantageous during primary infection because AdV nuclear trafficking precedes the expression of nc886 from AdV:nc886, it will be effective during secondary infection and thereafter. In summary, the incorporation of nc886 into AdV is not limited to gene delivery.

When we actually use nc886-expressing rAdV in clinical trials, we have to consider the potential adverse effects of nc886 itself, such as over-suppression of immunity, cancer development, and cell damage. In this regard, the rapid degradation of nc886 RNA is another major advantage. Considering that the half-life of nc886 is 1–2 h,[12,25,46] we expect nc886 expression to return to basal levels soon after AdV:nc886 clearance. nc886 is known to play an oncogenic role by inhibiting Dicer to suppress the microRNA (miRNA) pathway.[34] However, miRNAs are usually stable and their role in regulating target genes is mostly fine-tuning. Therefore, it is hard to imagine a situation where a transient increase in nc886 leads to cancer development by affecting the miRNA pathway. Although our previous study reported the inhibitory role of nc886 on cell proliferation by arresting cells in the G1 stage,[24] this would not be a problem because most of the cells targeted by AdV:nc886 in gene therapy will be non-proliferating cells in the G0 stage.

In summary, we have provided proof-of-concept that nc886-expressing rAdV is an improved gene delivery vehicle. The reduced cytotoxicity allows the dose of rAdV administered to be increased when higher expression of a therapeutic transgene is required. On the other hand, if cytotoxicity is a concern, the dose of rAdV can be reduced because transgene expression is higher at the same dose of AdV when nc886-expressing rAdV is used. In the future, our goal is to construct an nc886-expressing therapeutic rAdV, move it into clinical trials, and ultimately use it in patients. These efforts toward the clinic should be accompanied by in-depth basic research to elucidate the interaction between AdV and nc886 in immune responses, which would be complex and different in diverse cell types or among human individuals.

MATERIALS AND METHODS

AdV experiments

AdV5 is a wild-type hAdV (species C serotype 5, accession number GenBank: AY339865.1)[47] and was obtained from American Type Culture Collection (ATCC) (Manassas, VA). AdV:nc886 was constructed and generated by inserting a U6:nc886 cassette between E3 12.5k and U Exon in the E3 region of the parental AdV5/35 virus. AdV5/35 is our laboratory stock and was constructed by replacing the fiber knob domain of the AdV5 capsid with the fiber knob of the species B AdV35 (described in detail in Do et al.[26]). AdV virions were propagated in HEK293 cells and purified using an Adeno-X Maxi Purification Kit (Takara Bio USA, Mountain View, CA). AdV infection to cells in culture was done as follows; addition of AdV at indicated MOI in serum-free medium, incubation for 2 h at 37°C, and replacement with fresh medium containing 10% fetal bovine serum (FBS). For AdV infection to mice, 3.2×10^9 virus particles (or the corresponding volume of the elution buffer in the Adeno-X Maxi Purification Kit, for no-virus control) were tail-vein injected per mouse. The number of virus particles was calculated by qPCR together with titrating amounts of purified AdV DNA as a standard.

Cell culture and other reagents

RAW 264.7 and AML12 cell lines were purchased from ATCC and HEK293 was our laboratory stock. From the RAW 264.7 cells, we generated an nc886-expressing cell line as described in Lee et al.[14] In brief, we PCR-amplified a 649-nt fragment containing the nc886 gene and its flanking sequences and inserted it into pCAGGS-GFP plasmid, resulting in a plasmid named "pCAGGS-GFP/886." pCAGGS-GFP vector was originally derived from pCAGGS-Neo by inserting a gene encoding green fluorescent protein (GFP). These constructs were used to establish the RAW:vector and RAW:nc886 cell lines. The transfections were carried out using Lipofectamine 2000 reagent (Invitrogen, Carlsbad, CA), and clones were selected in the presence of G418 according to standard protocols. From the HEK293T cell line, we generated an nc886-expressing cell line as described in Im et al.[24] In short, we first generated an nc886-expressing plasmid, named "pLPCX-U6:nc886" by inserting a 101-nt long nc886 DNA fragment into control vector "pLPCX-U6" and transfected these plasmids into HEK293T cells by Lipofectamine 2000 reagent (Invitrogen), isolated clones by a standard laboratory protocol, and established 293T-vector and 293T-U6:nc886. Nthy-ori 3-1 and its derivative KO cell line are described in Lee et al.[22] In brief, Cas9-expressing plasmid ("hCas9"), in combination with guide RNA expression plasmids ("pCR sgPKR-1a" for PKR-KO to induce a frameshift of the PKR open reading frame or "pCR sg886-164" and "pCR sg886 + 15" for nc886-KO to delete the nc886 RNA region and the flanking sequences) was transfected by using Lipofectamine 2000 (Life Technologies) and clones were selected using G418 according to standard protocols.

Ruxolitinib was purchased from Sellekchem (Houston, TX). Caspase-3, PARP, and β-actin antibodies were purchased from Cell Signaling Technology (Danvers, MA).

Animal experiments

C57BL/6 male and female mice aged 6 weeks were obtained from Orient Bio (Seongnam, Korea). All animal experiments were performed in specific pathogen-free facilities and under the conditions of the Guidelines for the Association for Assessment and Accreditation of Laboratory Animal Care (AAALAC). All animal procedures were performed according to the National Cancer Center (NCC) guidelines for the care and use of laboratory animals. The protocol was approved by the Committee on the Ethics of Animal Experiments of the NCC (permit no. NCC-22-742-003).

The schedule for AdV injection and sacrifice is shown in Figure 3A. Mouse blood samples were collected from the orbital venous sinus just before sacrifice. Blood sera were isolated for measurement of hepatotoxicity markers GOT and GPT using an Asan GOT (or GPT) Assay kit, according to the manufacturer's instructions (Asan Pharm, Seoul, Korea). After sacrifice, livers were collected, and liver aliquots were cryopreserved for RNA isolation or fixed in 10% neutral buffered formalin for liver paraffin section embedding. Tissue section embedding in paraffin and H&E staining were commissioned to the histopathology laboratory of the NCC. For pathological analysis, spotty necrosis cluster numbers in liver tissues were manually counted from scan images of H&E stain slides at 4× magnification.

RNA isolation and measurement

Total RNA from cells and tissues were isolated by TRIzol reagent (Life Technologies, Carlsbad, CA). Northern hybridization was done as described previously.[12] cDNA was synthesized using a SuperScript III CellsDirect cDNA Synthesis Kit (Thermo Fisher Scientific; Waltham, MA) and real-time PCR was done using a LightCycler 480 SYBR Green I MasterMix (Roche, Penzberg, Germany) and LightCycler 480 Instrument II (Roche). When AdV mRNAs were measured, a reaction without reverse transcriptase ("no RT reaction") was done in parallel with a cDNA synthesis reaction ("+ RT reaction") to ensure that the PCR amplification was from RNA but not from AdV DNA. PCR values from no RT reaction were used as a baseline for the corresponding value of + RT reaction. Primer and probe sequences are summarized in Table S6).

Cell viability assay

The 3-(4,5-dimethylthiazol-2-yl)-2,5-diphenyltetrazolium bromide (MTT) assay was done with CellTiter 96 Non-Radioactive Cell Proliferation Assay (Promega, Madison, WI), according to the manufacturer's protocol.

Flow cytometric analysis of apoptotic cells

The FITC-Annexin V Apoptosis Detection Kit (BD Bioscience, Heidelberg, Germany) was used according to the manufacturer's protocol and cells were analyzed by flow cytometry using FACSVerse (BD Bioscience).

Statistical analysis

Statistical significance in most experiments (PCR, MTT, enzymatic assays) was expressed as standard deviation (SD) and p value using unpaired Student's t test. Further details are provided in the figure legends.

DATA AND CODE AVAILABILITY

All data from this study are included in this article or are available upon request. Raw RNA-seq data will be deposited in a public database upon acceptance of this manuscript.

SUPPLEMENTAL INFORMATION

Supplemental information can be found online at https://doi.org/10.1016/j.omtn.2024.102270.

ACKNOWLEDGMENTS

We thank Drs. Dae-Sik Lim (the Korea Advanced Institute of Science and Technology, Korea) and Eun Jung Park (the NCC, Korea) for helpful discussion. This work was supported by grants from the National Cancer Center, Korea (NCC-2210320 and NCC-2311362 to Y.S.L., NCC-2311361 to Y.-S.J.).

AUTHOR CONTRIBUTIONS

Conducting experiments, E.S., H.-H.L., S.R., S.-P.S., W.R.I., E.C., B.K.C., J.J.J., B.-H.C., and S.-J.L.; data analysis, E.S., H.-H.L., E.K.H., Y.K., T.-J.A., J.-L.P., S.-Y.K., Y.S.L., and S.-J.L.; conceptualization, E.S., Y.-S.L., I.-H.K., Y.S.L., and S.-J.L.; writing – original draft, E.S., H.-H.L., Y.S.L., and S.-J.L.; writing – review & editing, E.S., Y.-S.L., Y.S.L., and S.-J.L.; project administration, Y.-S.L., Y.-S.J., Y.S.L., and S.-J.L.; funding acquisition, Y.-S.J., I.-H.K., and Y.S.L.; supervision, Y.S.L.

DECLARATION OF INTERESTS

The authors declare no competing interests.

REFERENCES

1. Wold, W.S., and Toth, K. (2013). Adenovirus vectors for gene therapy, vaccination and cancer gene therapy. Curr. Gene Ther. *13*, 421–433. https://doi.org/10.2174/15665232113666131125095046.

2. Lee, C.S., Bishop, E.S., Zhang, R., Yu, X., Farina, E.M., Yan, S., Zhao, C., Zheng, Z., Shu, Y., Wu, X., et al. (2017). Adenovirus-Mediated Gene Delivery: Potential Applications for Gene and Cell-Based Therapies in the New Era of Personalized Medicine. Genes Dis. *4*, 43–63. https://doi.org/10.1016/j.gendis.2017.04.001.

3. Jaffe, H.A., Danel, C., Longenecker, G., Metzger, M., Setoguchi, Y., Rosenfeld, M.A., Gant, T.W., Thorgeirsson, S.S., Stratford-Perricaudet, L.D., Perricaudet, M., et al. (1992). Adenovirus-mediated *in vivo* gene transfer and expression in normal rat liver. Nat. Genet. *1*, 372–378. https://doi.org/10.1038/ng0892-372.

4. Xia, E., Zhang, Y., Cao, H., Li, J., Duan, R., and Hu, J. (2019). TALEN-Mediated Gene Targeting for Cystic Fibrosis-Gene Therapy. Genes *10*, 39. https://doi.org/10.3390/genes10010039.

5. Muruve, D.A. (2004). The innate immune response to adenovirus vectors. Hum. Gene Ther. *15*, 1157–1166. https://doi.org/10.1089/hum.2004.15.1157.

6. Atasheva, S., and Shayakhmetov, D.M. (2022). Cytokine Responses to Adenovirus and Adenovirus Vectors. Viruses *14*, 888. https://doi.org/10.3390/v14050888.

7. Schoggins, J.W. (2019). Interferon-Stimulated Genes: What Do They All Do? Annu. Rev. Virol. *6*, 567–584. https://doi.org/10.1146/annurev-virology-092818-015756.

8. Schoggins, J.W., Wilson, S.J., Panis, M., Murphy, M.Y., Jones, C.T., Bieniasz, P., and Rice, C.M. (2011). A diverse range of gene products are effectors of the type I interferon antiviral response. Nature *472*, 481–485. https://doi.org/10.1038/nature09907.

9. Chawla-Sarkar, M., Lindner, D.J., Liu, Y.F., Williams, B.R., Sen, G.C., Silverman, R.H., and Borden, E.C. (2003). Apoptosis and interferons: role of interferon-stimulated genes as mediators of apoptosis. Apoptosis *8*, 237–249. https://doi.org/10.1023/a:1023668705040.

10. Fausther-Bovendo, H., and Kobinger, G.P. (2014). Pre-existing immunity against Ad vectors: humoral, cellular, and innate response, what's important? Hum. Vaccines Immunother. *10*, 2875–2884. https://doi.org/10.4161/hv.29594.

11. Raper, S.E., Chirmule, N., Lee, F.S., Wivel, N.A., Bagg, A., Gao, G.P., Wilson, J.M., and Batshaw, M.L. (2003). Fatal systemic inflammatory response syndrome in a ornithine transcarbamylase deficient patient following adenoviral gene transfer. Mol. Genet. Metabol. *80*, 148–158. https://doi.org/10.1016/j.ymgme.2003.08.016.

12. Lee, K., Kunkeaw, N., Jeon, S.H., Lee, I., Johnson, B.H., Kang, G.Y., Bang, J.Y., Park, H.S., Leelayuwat, C., and Lee, Y.S. (2011). Precursor miR-886, a novel noncoding RNA repressed in cancer, associates with PKR and modulates its activity. RNA *17*, 1076–1089. https://doi.org/10.1261/rna.2701111.

13. Jeon, S.H., Lee, K., Lee, K.S., Kunkeaw, N., Johnson, B.H., Holthauzen, L.M., Gong, B., Leelayuwat, C., and Lee, Y.S. (2012). Characterization of the direct physical interaction of nc886, a cellular non-coding RNA, and PKR. FEBS Lett. *586*, 3477–3484. https://doi.org/10.1016/j.febslet.2012.07.076.

14. Lee, Y.S., Bao, X., Lee, H.H., Jang, J.J., Saruuldalai, E., Park, G., Im, W.R., Park, J.L., Kim, S.Y., Shin, S., et al. (2021). Nc886, a Novel Suppressor of the Type I Interferon Response Upon Pathogen Intrusion. Int. J. Mol. Sci. *22*, 2003. https://doi.org/10.3390/ijms22042003.

15. Golec, E., Lind, L., Qayyum, M., Blom, A.M., and King, B.C. (2019). The Noncoding RNA nc886 Regulates PKR Signaling and Cytokine Production in Human Cells. J. Immunol. *202*, 131–141. https://doi.org/10.4049/jimmunol.1701234.

16. Saruuldalai, E., Park, J., Kang, D., Shin, S.P., Im, W.R., Lee, H.H., Jang, J.J., Park, J.L., Kim, S.Y., Hwang, J.A., et al. (2022). A host non-coding RNA, nc886, plays a pro-viral role by promoting virus trafficking to the nucleus. Mol. Ther. Oncolytics *24*, 683–694. https://doi.org/10.1016/j.omto.2022.02.018.

17. Duncan, S.J., Gordon, F.C., Gregory, D.W., McPhie, J.L., Postlethwaite, R., White, R., and Willcox, H.N. (1978). Infection of mouse liver by human adenovirus type 5. J. Gen. Virol. *40*, 45–61. https://doi.org/10.1099/0022-1317-40-1-45.

18. Ginsberg, H.S., Moldawer, L.L., Sehgal, P.B., Redington, M., Kilian, P.L., Chanock, R.M., and Prince, G.A. (1991). A mouse model for investigating the molecular pathogenesis of adenovirus pneumonia. Proc. Natl. Acad. Sci. USA *88*, 1651–1655. https://doi.org/10.1073/pnas.88.5.1651.

19. Jogler, C., Hoffmann, D., Theegarten, D., Grunwald, T., Uberla, K., and Wildner, O. (2006). Replication properties of human adenovirus *in vivo* and in cultures of primary cells from different animal species. J. Virol. *80*, 3549–3558. https://doi.org/10.1128/JVI.80.7.3549-3558.2006.

20. Young, A.M., Archibald, K.M., Tookman, L.A., Pool, A., Dudek, K., Jones, C., Williams, S.L., Pirlo, K.J., Willis, A.E., Lockley, M., and McNeish, I.A. (2012). Failure of translation of human adenovirus mRNA in murine cancer cells can be partially overcome by L4-100K expression *in vitro* and *in vivo*. Mol. Ther. *20*, 1676–1688. https://doi.org/10.1038/mt.2012.116.

21. Chinnadurai, G. (1998). Control of Apoptosis by Human Adenovirus Genes. Semin. Virol. *8*, 399–408.

22. Lee, E.K., Hong, S.H., Shin, S., Lee, H.S., Lee, J.S., Park, E.J., Choi, S.S., Min, J.W., Park, D., Hwang, J.A., et al. (2016). nc886, a non-coding RNA and suppressor of PKR, exerts an oncogenic function in thyroid cancer. Oncotarget *7*, 75000–75012. https://doi.org/10.18632/oncotarget.11852.

23. Giberson, A.N., Davidson, A.R., and Parks, R.J. (2012). Chromatin structure of adenovirus DNA throughout infection. Nucleic Acids Res. *40*, 2369–2376. https://doi.org/10.1093/nar/gkr1076.

24. Im, W.R., Lee, H.S., Lee, Y.S., Lee, J.S., Jang, H.J., Kim, S.Y., Park, J.L., Lee, Y., Kim, M.S., Lee, J.M., et al. (2020). A Regulatory Noncoding RNA, nc886, Suppresses Esophageal Cancer by Inhibiting the AKT Pathway and Cell Cycle Progression. Cells *9*, 801. https://doi.org/10.3390/cells9040801.

25. Lee, Y.-S., and Lee, Y.S. (2023). nc886, an RNA Polymerase III-Transcribed Noncoding RNA Whose Expression Is Dynamic and Regulated by Intriguing Mechanisms. Int. J. Mol. Sci. *24*, 8533.

26. Do, M.H., To, P.K., Cho, Y.S., Kwon, S.Y., Hwang, E.C., Choi, C., Cho, S.H., Lee, S.J., Hemmi, S., and Jung, C. (2018). Targeting CD46 Enhances Anti-Tumoral Activity of Adenovirus Type 5 for Bladder Cancer. Int. J. Mol. Sci. *19*, 2694. https://doi.org/10.3390/ijms19092694.

27. Mathews, M.B. (1995). Structure, function, and evolution of adenovirus virus-associated RNAs. Curr. Top. Microbiol. Immunol. *199*, 173–187. https://doi.org/10.1007/978-3-642-79499-5_7.

28. Liu, Q., Zhou, S., Fan, C., Huang, W., Li, Q., Liu, S., Wu, X., Li, B., and Wang, Y. (2017). Biodistribution and residence time of adenovector serotype 5 in normal and immunodeficient mice and rats detected with bioluminescent imaging. Sci. Rep. *7*, 3597. https://doi.org/10.1038/s41598-017-03852-0.

29. Koizumi, N., Yamaguchi, T., Kawabata, K., Sakurai, F., Sasaki, T., Watanabe, Y., Hayakawa, T., and Mizuguchi, H. (2007). Fiber-modified adenovirus vectors decrease liver toxicity through reduced IL-6 production. J. Immunol. *178*, 1767–1773. https://doi.org/10.4049/jimmunol.178.3.1767.

30. Zheng, N., Wang, Y., Rong, H., Wang, K., and Huang, X. (2022). Human Adenovirus Associated Hepatic Injury. Front. Public Health *10*, 878161. https://doi.org/10.3389/fpubh.2022.878161.

31. Miyake, S. (1979). The mechanism of release of hepatic enzymes in various liver diseases. II. Altered activity ratios of GOT to GPT in serum and liver of patients with liver diseases. Acta Med. Okayama *33*, 343–358.

32. Hartman, Z.C., Appledorn, D.M., and Amalfitano, A. (2008). Adenovirus vector induced innate immune responses: impact upon efficacy and toxicity in gene therapy and vaccine applications. Virus Res. *132*, 1–14. https://doi.org/10.1016/j.virusres.2007.10.005.

33. Minamitani, T., Iwakiri, D., and Takada, K. (2011). Adenovirus virus-associated RNAs induce type I interferon expression through a RIG-I-mediated pathway. J. Virol. *85*, 4035–4040. https://doi.org/10.1128/JVI.02160-10.

34. Ahn, J.H., Lee, H.S., Lee, J.S., Lee, Y.S., Park, J.L., Kim, S.Y., Hwang, J.A., Kunkeaw, N., Jung, S.Y., Kim, T.J., et al. (2018). nc886 is induced by TGF-beta and suppresses the microRNA pathway in ovarian cancer. Nat. Commun. *9*, 1166. https://doi.org/10.1038/s41467-018-03556-7.

35. Shayakhmetov, D.M., Li, Z.Y., Ni, S., and Lieber, A. (2004). Analysis of adenovirus sequestration in the liver, transduction of hepatic cells, and innate toxicity after injection of fiber-modified vectors. J. Virol. *78*, 5368–5381. https://doi.org/10.1128/jvi.78.10.5368-5381.2004.

36. Schneider, W.M., Chevillotte, M.D., and Rice, C.M. (2014). Interferon-stimulated genes: a complex web of host defenses. Annu. Rev. Immunol. *32*, 513–545. https://doi.org/10.1146/annurev-immunol-032713-120231.

37. Huang, L., Heinloth, A.N., Zeng, Z.B., Paules, R.S., and Bushel, P.R. (2008). Genes related to apoptosis predict necrosis of the liver as a phenotype observed in rats exposed to a compendium of hepatotoxicants. BMC Genom. *9*, 288. https://doi.org/10.1186/1471-2164-9-288.

38. Febvre-James, M., Lecureur, V., Augagneur, Y., Mayati, A., and Fardel, O. (2018). Repression of interferon beta-regulated cytokines by the JAK1/2 inhibitor ruxolitinib in inflammatory human macrophages. Int. Immunopharm. *54*, 354–365. https://doi.org/10.1016/j.intimp.2017.11.032.

39. Bulcha, J.T., Wang, Y., Ma, H., Tai, P.W.L., and Gao, G. (2021). Viral vector platforms within the gene therapy landscape. Signal Transduct. Targeted Ther. *6*, 53. https://doi.org/10.1038/s41392-021-00487-6.

40. Naso, M.F., Tomkowicz, B., Perry, W.L., 3rd, and Strohl, W.R. (2017). Adeno-Associated Virus (AAV) as a Vector for Gene Therapy. BioDrugs *31*, 317–334. https://doi.org/10.1007/s40259-017-0234-5.

41. Cheng, Y., Zhang, Z., Gao, P., Lai, H., Zhong, W., Feng, N., Yang, Y., Yu, H., Zhang, Y., Han, Y., et al. (2023). AAV induces hepatic necroptosis and carcinoma in diabetic and obese mice dependent on Pebp1 pathway. EMBO Mol. Med. *15*, e17230. https://doi.org/10.15252/emmm.202217230.

42. Donsante, A., Miller, D.G., Li, Y., Vogler, C., Brunt, E.M., Russell, D.W., and Sands, M.S. (2007). AAV vector integration sites in mouse hepatocellular carcinoma. Science *317*, 477. https://doi.org/10.1126/science.1142658.

43. Sakurai, H., Tashiro, K., Kawabata, K., Yamaguchi, T., Sakurai, F., Nakagawa, S., and Mizuguchi, H. (2008). Adenoviral expression of suppressor of cytokine signaling-1 reduces adenovirus vector-induced innate immune responses. J. Immunol. *180*, 4931–4938. https://doi.org/10.4049/jimmunol.180.7.4931.

44. Xing, Z., Ohkawara, Y., Jordana, M., Graham, F.L., and Gauldie, J. (1997). Adenoviral vector-mediated interleukin-10 expression *in vivo*: intramuscular gene transfer inhibits cytokine responses in endotoxemia. Gene Ther. *4*, 140–149. https://doi.org/10.1038/sj.gt.3300371.

45. Peter, M., and Kühnel, F. (2020). Oncolytic Adenovirus in Cancer Immunotherapy. Cancers *12*, 3354. https://doi.org/10.3390/cancers12113354.

46. Park, J.L., Lee, Y.S., Song, M.J., Hong, S.H., Ahn, J.H., Seo, E.H., Shin, S.P., Lee, S.J., Johnson, B.H., Stampfer, M.R., et al. (2017). Epigenetic regulation of RNA polymerase III transcription in early breast tumorigenesis. Oncogene *36*, 6793–6804. https://doi.org/10.1038/onc.2017.285.

47. Nam, J.K., Lee, M.H., Seo, H.H., Kim, S.K., Lee, K.H., Kim, I.H., and Lee, S.J. (2010). The development of the conditionally replication-competent adenovirus: replacement of E4 orf1-4 region by exogenous gene. J. Gene Med. *12*, 453–462. https://doi.org/10.1002/jgm.1457.

OMTN, Volume *35*

Supplemental information

Adenovirus expressing nc886, an anti-interferon and anti-apoptotic non-coding RNA, is an improved gene delivery vector

Enkhjin Saruuldalai, Hwi-Ho Lee, Yeon-Su Lee, Eun Kyung Hong, Soyoun Ro, Yeochan Kim, TaeJin Ahn, Jong-Lyul Park, Seon-Young Kim, Seung-Phil Shin, Wonkyun Ronny Im, Eunjung Cho, Beom K. Choi, Jiyoung Joan Jang, Byung-Han Choi, Yuh-Seog Jung, In-Hoo Kim, Sang-Jin Lee, and Yong Sun Lee

Supplemental Figure

Figure S1

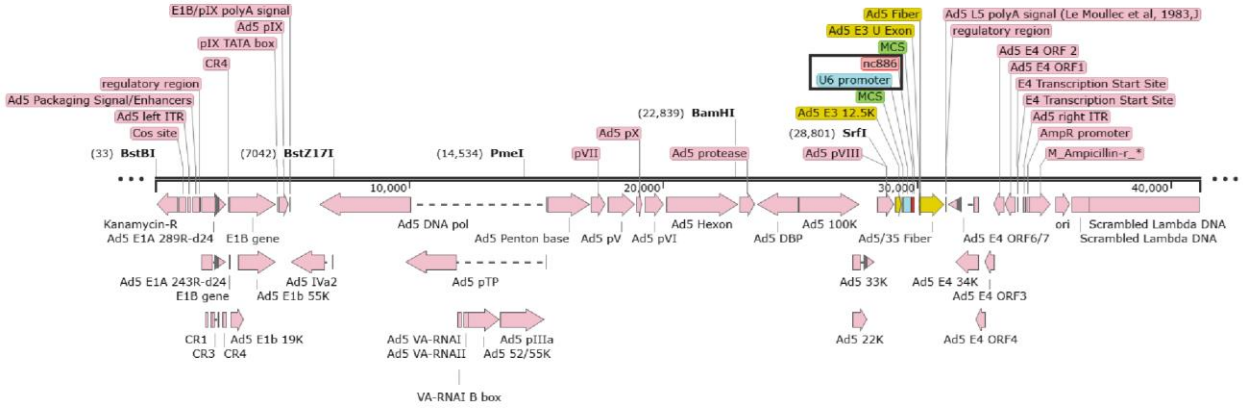

The full map of AdV:nc886

The U6:nc886 cassette region, which has been inserted into the parental AdV5/35 (see the main text for details), is highlighted in a box

List of Supplemental Tables

Table S1. Expression (TPM values from RNA-seq) of 376 ISGs at 6 hpi.

Table S2. Expression (TPM values from RNA-seq) of 376 ISGs at 24 hpi.

Table S3. Biocarta pathways: Z-scores relative to column B ("uninfected") samples

Table S4. Reactome pathways: Z-scores relative to column B ("uninfected") samples

Table S5. Gene Ontology Biological Process pathways: Z-scores relative to column C ("uninfected") samples

Table S6. Primers and probes used in this study

primer name	sequence (5' to 3')	comments
Hexon_2636-56	TTATGTCCATGGGCGCACTCA	forward primer for AdV Hexon qRT-PCR, qPCR
Hexon_2783-60	ACACGGACCACGTCAAAGACTTCA	reverse primer for AdV Hexon qRT-PCR, qPCR
Ad_VAI_142-22	TTGTCTGACGTCGCACACCTG	Northern probe for adenoviral ncRNA VA I
miR-886-3p as	AAGGGTCAGTAAGCACCCGCG	Northern probe and reverse primer for nc886 qRT-PCR
miR-886-5p sense	CGGGTCGGAGTTAGCTCAAGCGG	forward primer for nc886 qRT-PCR
Gapdh_774-96	CATCACTGCCACCCAGAAGACTG	forward primer for mouse Gapdh qRT-PCR
Gapdh_926-04	ATGCCAGTGAGCTTCCCGTTCAG	reverse primer for mouse Gapdh qRT-PCR
mIfit1-885-905	TTCTAAACAGGGCCTTGCAGG	forward primer for mouse Ifit1 qRT-PCR
mIfit1-1019-999	CTTGCACATTGTCCTGCCTTC	reverse primer for mouse Ifit1 qRT-PCR
mIfit2_658-78	AGCACTGCAGAGGTCTAAATG	forward primer for mouse Ifit2 qRT-PCR
mIfit2_788-68	GTAGACCCAAGCATAGTTTCC	reverse primer for mouse Ifit2 qRT-PCR
mXaf1_1484-504	CGCACACACACATGCTAACAT	forward primer for mouse Xaf1 qRT-PCR
mXaf1_1618-598	CTGGGTGGGGTACTATCAGAT	reverse primer for mouse Xaf1 qRT-PCR
IFIT1_3739-62	CCCCAAGAAAATCTCCAAATTTTG	forward primer for human IFIT1 qRT-PCR
IFIT1_3859-36	AATCTCTGTCCTACCTTCTTAAGG	reverse primer for human IFIT1 qRT-PCR
XAF1_897-920	GTTAGCTTCATCAAAAGGAAAACA	forward primer for human XAF1 qRT-PCR
XAF1_997-74	GAATGCCAGTGTTAAAAGTGAAAT	reverse primer for human XAF1 qRT-PCR
18S rRNA 281-300	CGGCTTTGGTGACTCTAGAT	forward primer for human 18S rRNA qRT-PCR
18S rRNA 381-362	GCGACTACCATCGAAAGTTG	reverse primer for human 18S rRNA qRT-PCR